

Challenges for cognitive decoding using deep learning methods

Armin W. Thomas ^{★,◇,*}, Christopher Ré [■], and Russell A. Poldrack ^{★,◇}

[★] Stanford Data Science, Stanford University, Stanford, CA, USA

[◇] Department of Psychology, Stanford University, Stanford, CA, USA

[■] Department of Computer Science, Stanford University, Stanford, CA, USA

*Correspondence: athms@stanford.edu (A. W. Thomas)

Keywords: cognitive decoding, deep learning, neuroimaging, explainable artificial intelligence,
transfer learning, robustness

In cognitive decoding, researchers aim to characterize a brain region's representations by identifying the cognitive states (e.g., accepting/rejecting a gamble) that can be identified from the region's activity. Deep learning (DL) methods are highly promising for cognitive decoding, with their unmatched ability to learn versatile representations of complex data. Yet, their widespread application in cognitive decoding is hindered by their general lack of interpretability as well as difficulties in applying them to small datasets and in ensuring their reproducibility and robustness. We propose to approach these challenges by leveraging recent advances in explainable artificial intelligence and transfer learning, while also providing specific recommendations on how to improve the reproducibility and robustness of DL modeling results.

22
23 **Glossary:**
24
25 **Cognitive state:** An unobservable construct of psychological theory that refers to a particular mental operation or content
26 and is often associated with specific observable behaviors.
27
28 **CV:** Computer vision (CV) is an area of artificial intelligence research, which aims to enable computers to derive
29 meaningful information from the visual world and to take actions based on that information.
30
31 **DL:** Deep learning (DL) describes a class of representation learning methods, which transform the input data in multiple
32 sequential steps (or layers), each applying stacks of simple, but nonlinear functions.
33
34 **fMRI:** Functional magnetic resonance imaging (fMRI) measures brain activity by detecting changes in activity
35 associated with changes in local blood flow.
36
37 **NLP:** Natural language processing (NLP) is an area of artificial intelligence research, which aims to enable computers
38 to derive meaningful information from human language and to take actions based on that information.
39
40 **Representation:** As used in computer science, a transform of some data in terms of a different set of features.
41
42 **XAI:** Explainable artificial intelligence (XAI) represents a class of methods, which aim to make the behavior of DL
43 methods understandable to human observers, for example, by relating the features of some input data to the respective
44 outputs of the model.
45

46 The promise of deep learning

47 Over the last decade, deep learning (**DL**; see Glossary and [1]) methods have
48 revolutionized many areas of research and industry with their ability to learn highly versatile
49 **representations** (or concepts) from complex data. A defining feature of DL methods is that they
50 sequentially apply stacks of many simple, but nonlinear, transforms to their input data, allowing
51 them to gain an increasingly abstracted view of the data. At each level of the transform, new
52 representations of the data are built by the use of representations from preceding layers. The
53 resulting high-level view of the data enables DL methods to capture complex nonlinearities,
54 associate a target signal with highly variable patterns in the data (e.g., when identifying objects in
55 images or transcribing audio recordings), and effectively filter out aspects of the data that are
56 irrelevant to the learning task at hand. A key driver for the empirical success of DL methods is that
57 they are able to autonomously learn these different levels of abstraction from sufficiently large
58 datasets, without the need for extensive data preprocessing or a prior understanding of the mapping
59 between input data and target signal.

60 This empirical success has recently sparked interest in the application of DL methods to
61 the field of neuroimaging, focused on cognitive decoding [2]. Here, researchers aim to understand
62 the mapping between a set of **cognitive states** (e.g., answering questions about a math problem vs.
63 a prose story) and the underlying brain activity by training some predictive model to identify these
64 states from measured brain activity [3]. At first sight, DL methods seem ideally suited for these
65 types of analyses, as the mapping between cognitive states and brain activity is often a priori
66 unknown, can be highly variable within [4] and between individuals [5], and is subject to spatial
67 and temporal non-linearities [6].

68 Yet, the application of DL methods to cognitive decoding analyses also raises several new
69 challenges for researchers who are interested in combining methods from both fields, namely, a
70 general lack of interpretability of DL methods, their overall demand for large training datasets,
71 and difficulties in ensuring the reproducibility and robustness of DL modeling results. Here, we
72 outline each of these challenges and present a set of solutions based on related empirical work and
73 recent methodological advances in both functional neuroimaging and machine learning research.

74 Opening up the black box

75 A key challenge for the application of DL models to functional neuroimaging data is the
76 black-box characteristic of DL models, whose highly non-linear nature deeply obscures the
77 relationships between input data and decoding decisions. Thus, even if a DL model accurately
78 decodes a set of cognitive states from functional neuroimaging data, it is not clear which particular
79 features of the data (or combinations thereof) support this decoding. To approach this challenge,
80 functional neuroimaging researchers have begun turning towards research on explainable artificial
81 intelligence (**XAI**; [7-9]), where techniques are being developed that aim to make the behavior of
82 DL models (and other intelligent artificial agents) understandable for human observers.

83 One line of research within this field seeks to explain the predictions of DL models by
84 relating these predictions to the features of the input data, thus, making the model interpretable for
85 human observers [10]. On a high level, these explanation techniques can be categorized into those
86 that aim to provide either a global or local explanation of the model's learned mapping between
87 input data and predictions [8,9]. Global explanations [11,12] are not tied to a specific data sample
88 and seek to provide insights into the characteristics of the data at large that influence the model's

89 predictions (e.g., by synthesizing the image for which the model is most certain that it depicts a
90 dog). Local explanations [12-29], on the other hand, are specific for a data sample and seek to
91 provide insights into the mapping between the features of the sample and the resulting prediction
92 of the model (e.g., by identifying those pixels of an image that the model views as evidence for
93 the presence of a dog). Further, explanation techniques can be categorized into those that can be
94 applied post-hoc to the predictions of an already trained model [11-26] and those that are integrated
95 into the training procedure, such that the model is self-explaining and designed a priori to provide
96 human-understandable insights into its learned mappings between data and predictions [27-31].

97 Here, we focus on local explanation approaches. We provide an overview of a set of
98 representative approaches to this type of XAI in Box 1. Of these approaches, sensitivity analysis
99 [12,22], backward decomposition [13-19,21,24], and attention mechanisms [27-29] are currently
100 most prominent in the functional neuroimaging literature on cognitive decoding with DL models
101 [32-40]. Sensitivity analysis seeks to explain the predictions of a DL model by identifying those
102 features of an input sample to which the model's prediction responds most sensitively. Backward
103 decompositions, on the other hand, seek to explain individual predictions by sequentially
104 decomposing these predictions in a backward pass into the contributions of the lower-layer model
105 units to these predictions, until the input space is reached and a contribution for each input feature
106 can be defined. Attention mechanisms, in contrast, are inspired by research in neuroscience on
107 perceptual attention [41] and aim to improve the predictive performance of a DL model by
108 focusing its computations on specific aspects of an input sample (through a set of attention
109 weights). Attention mechanisms are thus an integrated feature of the training procedure and cannot
110 be applied post-hoc to the predictions of trained models.

111 At first sight, the explanations of these three XAI techniques can be difficult for human
112 observers to distinguish, making it difficult to compare the quality of their explanations. To
113 approach this challenge, researchers in machine learning have started developing methods to
114 quantify the quality of these types of explanations [8,42-47]. One prominent approach is to test the
115 faithfulness of an explanation [8,42,44,46]. An explanation can generally be viewed as being faithful
116 [48] if it accurately captures the model's decision process and thereby identifies those features of
117 the input that are most relevant for the model's prediction. Accordingly, removing these features
118 from the input (e.g., in an occlusion analysis; [8,42,44]) should lead to a meaningful decline of the
119 model's predictive performance.

120

121 **Box 1. Exemplary approaches to local explainable artificial intelligence.**

122 We assume that the analyzed model represents some function $f(\cdot)$, mapping an input $x \in \mathbb{R}^D$ to some output $f(x): f(\cdot)$
123 $): \mathbb{R}^D \rightarrow \mathbb{R}$. The presented local explanation approaches $\eta(\cdot)$ seek to provide insights into this mapping by quantifying
124 the relevance r_d of each input feature $d \in D$ for $f(x): \eta(\cdot): \mathbb{R} \rightarrow \mathbb{R}^D$ (Fig. I).

125

126 **Occlusion analysis** [20,24,25]: The occlusion analysis is a perturbation analysis, which identifies r_d by occluding x_d in
127 the data and measuring the resulting effect on $f(x): r_d = \Delta f(x) = f(x) - f(x \times o_d)$. Here, o_d indicates an occlusion
128 vector (e.g., $o_d \in [0,1]^D$), and \times the element-wise product.

129

130 **Interpretable local surrogate model** [26]: A local surrogate model is an interpretable model that is used to explain
131 black-box model predictions by training it to approximate these predictions. In the LIME algorithm [26], r is quantified
132 by approximating $f(x)$ for a specific x with an interpretable model $g(\cdot)$, e.g., a linear model, where $g(x) = w^T x$, and
133 which is trained by the use of a set of perturbed versions Z of x (e.g., through occlusion): $\min_w \sum_{z \in Z} \pi_x(z) (f(z) -$
134 $g(z))^2$. Here, π_x represents some similarity function weighting each $z \in Z$ by its similarity to x , while r_d is given by
135 the corresponding linear model weight $w_d: r_d = w_d$.

136

137 **Sensitivity analysis** [12,22]: Sensitivity analysis defines r as the locally evaluated partial derivative of $f(x): r =$
138 $f'(x) = (\frac{\partial f(x)}{\partial x})^2$. Accordingly, relevance is assigned to those features x_d to which $f(x)$ responds most sensitively.

139

140 **Backward decomposition** [13-19,21,24]: Backward decompositions make specific use of the graph structure of DL
141 models by sequentially decomposing $f(x)$ in a backward pass through the model until the input space is reached. A
142 prominent example is the layer-wise relevance propagation (LRP; [13]) technique: Let i and j be the indices of two
143 model units in two successive layers, r_j the relevance of unit j for $f(x)$, and $r_{i \leftarrow j}$ the part of r_j that is redistributed from
144 j to i during the backward decomposition. To redistribute relevance between layers, several rules have been proposed
145 [49,50], which generally follow from: $r_i = \sum_j \frac{a_i w_{ij}}{\sum_i a_i w_{ij}} r_j$, where a and w represent the input and weights of unit i .

146 Importantly, LRP assumes that relevance is conserved between layers, such that $\sum_i r_{i \leftarrow j} = r_j$, $r_i = \sum_j r_{i \leftarrow j}$, and $\sum_d r_d =$
147 $\dots = \sum_i r_i = \sum_j r_j = f(x)$.

148

149 **Attention mechanism** [27-29]: In contrast to the other presented explanation approaches, attention mechanisms are built
150 into and trained with a DL model. Their goal is to help the model focus its computations on specific aspects of x by the
151 use of attention glimpses $\gamma \in \mathbb{R}^D$. These glimpses can be implemented by the use of a separate model, which predicts an
152 attention weight α_d for each x_d [27,28]. These weights are multiplied with the input ($\gamma = \alpha \times x$) and the resulting
153 glimpse is forwarded to the remaining parts of the model (instead of x). Attention weights are often also interpreted as
154 an estimate of relevance, such that $r_d = \alpha_d$ [32,42,43].

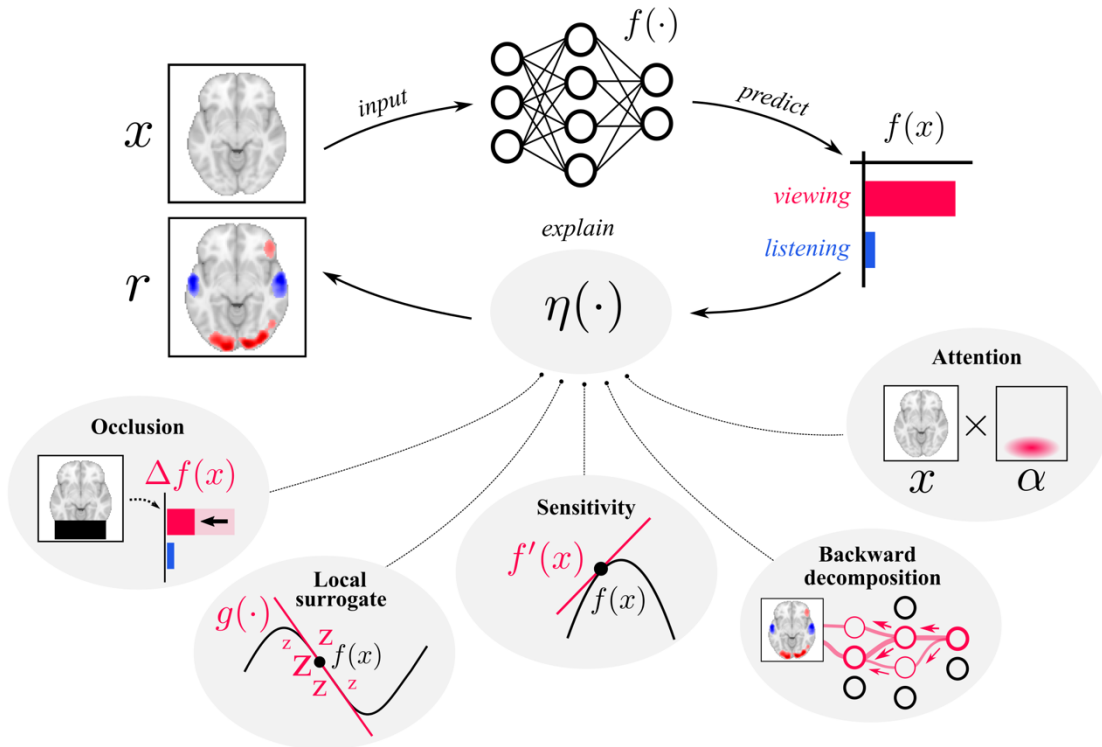


Figure I. Exemplary approaches to local explainable artificial intelligence.

155
156
157

158 By the use of this test, researchers in computer vision (CV; [44]) and natural language
 159 processing (NLP; [42,43]) have compared the fidelity of explanations resulting from sensitivity
 160 analysis and backward decomposition. This work has shown that backward decompositions
 161 generally perform better at identifying those features of the input that are most relevant for model
 162 predictions. Intuitively, this makes sense, as backward decompositions seek to directly quantify
 163 the contribution of each input feature to a specific model prediction. Sensitivity analysis, in
 164 contrast, does not evaluate the prediction itself but its local slope, thus identifying features that
 165 make the model more or less certain of its prediction, regardless of their actual contribution to the
 166 prediction. Similarly, related empirical work [42,43,46] has demonstrated that standard attention
 167 mechanisms do not provide faithful explanations of the predictions of DL models, as they fail to
 168 identify features of the input that are relevant for the prediction. Attention mechanisms are
 169 designed to improve the predictive performance of a DL model by enhancing certain aspects of
 170 the input while fading out others. Their decisions on how to weight each input feature are thus
 171 tailored to the subsequent computations of the DL model and not designed to identify the relevance
 172 of each feature for the prediction.

173 While functional neuroimaging researchers have also used the occlusion analysis to
174 analyze cognitive decoding models (in “virtual lesion analyses”; [35,51]), these applications have
175 been mostly limited to linear models and to testing whether specific brain regions, which received
176 large weights in a linear model, are actually necessary for an accurate decoding. For functional
177 neuroimaging data, occlusion analyses generally require a clear prior hypothesis on which features
178 (or brain regions) of the input will be tested (e.g., resulting from other research or other explanation
179 analyses), as randomly dropping out individual feature values will otherwise not account for the
180 strong spatial correlation structure inherent to these data.

181 Taken together, we thus generally recommend the application of backward decompositions
182 to analyze cognitive decoding decisions of DL models (see Box 2 for specific recommendations).

183 In addition to selecting an XAI technique, functional neuroimaging researchers interested
184 in understanding the decoding decisions of deep cognitive decoding models are also faced with
185 the task of analyzing the resulting dataset of explanations (which is generally equal in size to the
186 original input data, as one explanation is obtained for each input sample). Many current empirical
187 applications of XAI in cognitive decoding simply average individual explanations or analyze them
188 with standard linear models [32-34,36-38]. These types of linear analyses, however, are limited in
189 their ability to identify any non-linear mappings between brain activity and cognitive states that a
190 DL model might have learned. This problem has been similarly encountered in machine learning
191 research. Here, researchers have instead advocated for the application of automated, non-linear,
192 and data-driven approaches to identifying the learned decision behaviors of DL models from
193 explanation data (e.g., through t-distributed stochastic neighbor embedding; [52]). In functional
194 neuroimaging, current methods from network neuroscience [53] also seem highly promising for
195 analyzing explanation data, by identifying the individual units (e.g., brain regions) of the learned
196 mappings between brain activity and decoded cognitive states as well as the dynamics of their
197 interactions.

198

199 **Box 2. Recommended XAI approaches for cognitive decoding.**

200 We generally recommend the application of backward decompositions (see Box 1 and [13-19,21,24]) to analyze the
 201 contribution of individual input features to the cognitive decoding decisions of DL models. Below, we provide three
 202 specific recommendations for XAI approaches for cognitive decoding:

203

204 **LRP** [13]: An overview of LRP is provided in Box 1. While several rules have been proposed to redistribute relevance
 205 r between units i and j of two successive layers [13,49,50], recent empirical work has shown that a composite of these
 206 rules is best-suited for CV models [49,50]. Specifically, this work suggest combining the LRP-0 rule ($r_i = \sum_j \frac{a_i w_{ij}}{\sum_i a_i w_{ij}} r_j$,
 207 where a and w represent the input and weights of unit i) for layers closer to the output, with the LRP- ϵ rule ($r_i =$
 208 $\sum_j \frac{a_i w_{ij}}{\epsilon + \sum_i a_i w_{ij}} r_j$ with $1e^{-4} \leq \epsilon < 1$) for middle layers, and the LRP- γ rule ($r_i = \sum_j \frac{a_i (w_{ij} + \gamma w_{ij}^+)}{\sum_i a_i (w_{ij} + \gamma w_{ij}^+)} r_j$, where γ controls
 209 positive contributions and is generally $0 < \gamma$) for layers closer to the input. A TensorFlow implementation of LRP is
 210 provided by iNNvestigate [54], while Captum [55] provides PyTorch implementation.

211

212 **Deep learning important features (DeepLIFT)** [16]: DeepLIFT seeks to explain the contribution of model unit i to
 213 prediction $f(x)$ by comparing the unit's current activation a_i to a reference activation a_i^0 , which results from a reference
 214 input x^0 [16]. The reference input x^0 should be neutral and preserve only those properties of the input that are not
 215 considered relevant to the decoding problem while removing properties that are considered relevant (e.g., for MNIST,
 216 an all-zero reference is recommended, as this is the MNIST background). For functional neuroimaging data, we thus
 217 recommend an all-zero reference, a reference that adds noise to the input as well as a reference involving samples from
 218 other decoding classes (e.g., their average). We further recommend using multiple references to increase robustness
 219 towards specific reference choices [23]. A TensorFlow implementation of DeepLIFT can be found at
 220 github.com/kundajelab/deeplift and github.com/slundberg/shap, while Captum [55] provides a PyTorch implementation.

221

222 **Integrated gradients (IG)** [15]: The integrated gradients (IG) technique is closely related to both LRP and DeepLIFT
 223 [56]. IG is applicable to any differentiable model and defines relevance r_d of input feature d for prediction $f(x)$ by
 224 integrating the gradient $f'(x)$ along some trajectory in the input space connecting a reference point x^0 to the current
 225 input x : $r_d = (x_d - x_d^0) \int_{\alpha=0}^1 \frac{\delta f(x^0 + \alpha(x - x^0))}{\delta x_d} d\alpha$. Similar to DeepLIFT, the authors recommend an all-zero reference or
 226 the addition of noise to the input [14,57], while an average over multiple references is also possible [57]. A tutorial on
 227 how to use IG in TensorFlow can be found at tensorflow.org/tutorials/interpretability/integrated_gradients, while
 228 Captum [55] provides a PyTorch implementation.

229

230 Leveraging public data

231 A second major challenge for DL models in functional neuroimaging research is the high
232 dimensionality and low sample size of conventional functional neuroimaging datasets. A typical
233 functional Magnetic Resonance Imaging (**fMRI**) dataset contains a few hundred volumes for each
234 of tens to hundreds of individuals, while each volume contains several hundred thousand voxels
235 (or dimensions). Current state-of-the-art DL models, in contrast, can easily contain many hundred
236 million parameters [58,59], while recent language models have pushed this boundary even further
237 with many billion parameters [60-62]. In most cases, DL models thus contain many more trainable
238 parameters than there are samples in their training data. While this vast overparameterization
239 represents a key element to the empirical success of DL models, by enabling them to find near-
240 perfect solutions for most standard learning tasks [63,64] and to generalize well between datasets
241 [62,65,66], it also represents one of the biggest challenges for their application in fields where data
242 are scarce, as the performance of DL models is strongly dependent on the amount of available
243 training data [61,67].

244 To approach this challenge, researchers have developed many methods that aim to improve
245 the performance of DL methods in smaller datasets (e.g., [68-71]). One of these methods, with
246 strong empirical success, is transfer learning [71]. The goal of transfer learning is to leverage the
247 knowledge about a mapping between input data and a target variable that can be learned from one
248 dataset (i.e., the source or upstream domain) to subsequently improve the learning of a similar
249 mapping in another dataset of a related domain (i.e., the target or downstream domain). Knowledge
250 is typically transferred in the form of the parameters that a model has learned in the source domain
251 and that are then used to initialize the model (or parts of the model) when beginning learning in
252 the target domain. Transfer learning has been especially successful in CV and NLP, where large
253 publicly available datasets exist (e.g., [72,73] and <http://www.commoncrawl.org>). Here, DL
254 models are first pre-trained on these large datasets (e.g., to classify objects in images) and
255 subsequently fine-tuned on smaller datasets of a related target domain (e.g., to classify brain
256 tumors in medical imaging; [74]). Computationally, pre-training can aid subsequent optimizations
257 by placing the parameters near a local minimum of the loss function [75] and by acting as a
258 regularizer [76]. Pre-trained models generally exhibit faster learning and higher predictive
259 accuracy, while also requiring less training data when compared to models that are trained from

260 scratch [61,65,66,71,75-78]. The benefits of pre-training can diminish, however, with increasing
261 size of the target dataset [61] and as the overall differences between source and target learning task
262 and/or domain increase [79,80].

263 Over recent years, the field of functional neuroimaging has experienced a similar increase
264 in the availability of public datasets, which are provided by large neuroimaging initiatives as well
265 as individual researchers [81]. In addition, several efforts have been made to standardize the
266 organization (e.g., [82,83]) and preprocessing (e.g., [84]) of functional neuroimaging data. These
267 developments have paved the way for the field of functional neuroimaging to enter a big data era,
268 allowing for the application of transfer learning.

269 First empirical evidence indicates that transfer learning between individuals [85-87],
270 experiment tasks [36, 37, 39,88], and datasets [89-92] is possible and that pre-training generally
271 improves the performance of DL models when applied to conventional fMRI datasets
272 [36,85,86,88,89,91]. Most of this work has utilized traditional supervised learning techniques
273 during pre-training, by assigning a cognitive state to each sample in the data and training a
274 decoding model to identify these states from the data (see Box 3). While this is a fruitful approach
275 to decoding analyses within individual neuroimaging datasets, it is often difficult to extend to
276 analyses across many datasets. In spite of several attempts (e.g., [93,94]), functional neuroimaging
277 research has yet to widely adopt standardized definitions of cognitive states. Without this type of
278 standardization, it is often unclear whether two experiments from two separate laboratories elicit
279 the same or different sets of cognitive states. Imagine the following experiments: In the first,
280 participants read aloud a sequence of sentences and are then asked to repeat the last word of each
281 sentence [95]. In the second, participants first hear a sequence of letters and digits and are then
282 asked to report back the letters and digits in alphabetical and numerical order respectively (the
283 letter–number sequencing task; [96]). While both experiments label the associated cognitive state
284 as “working memory”, one could argue that the experiments in fact elicit two distinct cognitive
285 states, as one solely requires temporarily storing information while the other also requires active
286 manipulation of this information.

287 This problem of imprecisely labeled data has been similarly encountered in machine
288 learning research. Here, researchers have developed weakly supervised learning techniques, which
289 aim to train DL models with noisy or incomplete data labels [97]. One prominent weak supervision
290 approach is data programming (see Box 3 and [98,99]), which seeks to alleviate the cost of

291 manually labeling large datasets by the use of simple labeling functions. These functions
292 automatically label subsets of the data by implementing simple domain heuristics of subject matter
293 experts (e.g., label a YouTube text comment as Spam if it contains a URL or the words “check this
294 out”). The generated labels are then used to train DL models in a supervised manner. Importantly,
295 data programming frameworks account for noise and conflicts that can arise from the automatic
296 labeling by representing the labeling process as a generative model [98,99]. Recent empirical work
297 has demonstrated that this type of weak supervision can be successfully used for the classification
298 of unlabeled medical imaging data (e.g., radiography or computer tomography data; [100]), by
299 designing labeling functions that extract labels from the accompanying medical text reports. A
300 similar approach could be fruitful to generate standardized labels of cognitive states (e.g.,
301 according to the Cognitive Atlas; [94]) by applying these types of automatic labeling functions to
302 the accompanying publication texts (e.g., label an fMRI scan as “visual perception” if the
303 publication text contains the words “viewed” or “viewing” in the Methods section).

304 An alternative approach, with strong recent empirical success, is unsupervised learning
305 (see Box 3 and [101,102]). Unsupervised learning does not consider any labeling and instead trains
306 models to autonomously learn meaningful representations of the data. These learned
307 representations can then be used to improve learning in a related target domain. Two prominent
308 examples of unsupervised learning are contrastive and generative learning [103]. Both learn a
309 representation of the data by training an encoder model to project the data into a lower-dimensional
310 representation, which preserves relevant information. In contrastive learning [104], the encoder
311 model is trained by the use of an additional discriminator model, which aims to determine the
312 similarity of a pair of data samples based on their projection through the encoder model. During
313 training, positive pairs of samples are created by randomly augmenting the same data sample twice
314 (e.g., different views of the same image), while negative pairs are created by augmenting two
315 different data samples. Generative learning [105], in contrast, trains the encoder model by the use
316 of an additional decoder model, which aims to reconstruct the original data sample from the lower-
317 dimensional representation of the encoder model.

318

319 **Box 3. Approaches to pre-training.**

320 Transfer learning aims to improve the performance of model $f(\cdot)$ in a target learning task T_T in a target domain D_T by
 321 leveraging knowledge that can be learned by *pre-training* $f(\cdot)$ in a related source learning task T_S and source domain D_S
 322 [71]. Knowledge is generally transferred through a set of model weights W that $f(\cdot)$ has learned during pre-training. A
 323 domain D is defined by a feature space X with samples $x \in \mathbb{R}^N$ whose N feature values are characterised by some
 324 probability distribution $P(X)$. Given a domain, a learning task T consists of learning some mapping between a label
 325 space Y and the associated feature space X , by training $f(\cdot)$ to accurately predict the target values $y \in Y$ assigned to the
 326 samples $x \in X$ in a dataset $A = \{(x_i, y_i), \dots, (x_m, y_m)\}$, such that $f(x_i) \approx y_i$. Here, we describe three learning tasks
 327 (Fig. I), which enable $f(\cdot)$ to learn in a source domain, when the target values y of a source dataset A_S are either fully
 328 accessible, noisy or incomplete, or not accessible.

329

330 **Supervised learning** [106]: In supervised learning, the target values $y \in A_S$ are fully accessible and can be used to train
 331 $f(\cdot)$, for example, by minimizing the distance between $f(x)$ and y : $\min_W \sum_{\{x_i, y_i\} \in A_S} (y_i - f(x_i))^2$.

332

333 **Weakly supervised learning** [97]: In weakly supervised learning, the target values $y \in A_S$ are noisy or incomplete. A
 334 prominent example of weak supervision is data programming [98], where noisy target values \hat{y} are generated for an
 335 unlabeled source dataset by the use of user-specified labeling functions. These labeling functions implement domain
 336 heuristics of subject matter experts (e.g., label a chest radiograph as “abnormal” if the corresponding medical text report
 337 contains a word with the prefix ‘pneumo’; [100]). The generated target values are then used to train $f(\cdot)$ in a supervised
 338 way.

339

340 **Unsupervised learning** [101,102]: In unsupervised learning, the target values $y \in A_S$ are not accessible. Instead, a new
 341 learning task is devised, which requires $f(\cdot)$ to independently learn a representation of the data in the source domain.
 342 Two prominent unsupervised learning strategies are contrastive and generative learning. Both treat $f(\cdot)$ as an encoder
 343 model, which is trained to project the samples $x \in A_S$ into a lower-dimensional representation that preserves relevant
 344 information: $f(\cdot): \mathbb{R}^N \rightarrow \mathbb{R}^L$ (where $L < N$). In contrastive learning [104], $f(\cdot)$ is trained by the use of an additional
 345 discriminator model $d(\cdot): \mathbb{R}^L \rightarrow \mathbb{R}$, which learns to determine the similarity of a pair of data samples based on the
 346 encoder’s projection. During training, a set of augmented versions $\{\hat{x}\}$ of the data samples $x \in A_S$ is created and the
 347 discriminator’s task is to identify pairs $\{\hat{x}_k, \hat{x}_j\}$ that result from the same sample x_i . In generative learning [105], $f(\cdot)$ is
 348 trained by the use of an additional decoder model $d(\cdot): \mathbb{R}^L \rightarrow \mathbb{R}^N$, which aims to reconstruct the original data sample
 349 from the encoder’s projection: $d(f(x_i)) \approx x_i$.

350

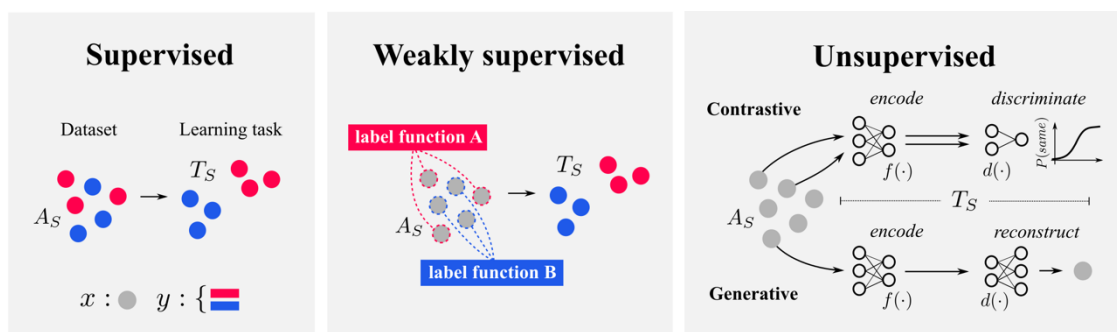


Figure I. Illustration of three exemplary source learning tasks (T_S), given some source dataset (A_S).

351
352
353

354 Ensuring reproducibility and robustness

355 Recent work in functional neuroimaging has exposed the high flexibility of its standard
356 analysis workflows, leading to substantial variability in results and scientific conclusions [107]. In
357 light of these issues, various efforts have been made to improve the standardization and
358 reproducibility of functional neuroimaging analyses (e.g., [82,84]). DL research is currently facing
359 similar concerns, with model performances that are often hard to reproduce [108-111] and not
360 robust to the diversity of real-world data [79,112-122]. Functional neuroimaging researchers who
361 are interested in applying DL methods to cognitive decoding analyses are thus faced with
362 additional challenges for the reproducibility and robustness of their work, which arise at the
363 intersection of both fields.

364 Methodological progress in DL research is often driven by a hunt for state-of-the-art
365 performances in benchmarks (see <http://www.paperswithcode.com/sota>), that is, by whether a new
366 methodology outperforms existing ones in pre-defined test datasets. While this approach has
367 helped the field of DL to evolve fast and quickly develop accurate models, it has also established
368 a research culture that often sacrifices scientific rigor for maximal performance metrics [123,124],
369 not unlike the “p-hacking” phenomenon in null hypothesis testing [125].

370 A central argument for predefined test datasets is that all models should be compared on
371 the same grounds (i.e., the same sets of training and testing samples). Yet, these types of point
372 estimates are often insufficient to determine whether a model actually outperforms others in new
373 data. Recent empirical work has demonstrated, for example, that the convergence of DL models
374 and thereby their final performance in a test dataset is dependent on many non-deterministic factors

375 of the training, such as random weight initializations and random shufflings or augmentations of
376 the data during training [110,111,126], as well as the specific choices for hyper-parameters, such
377 as the specification of individual model layers and optimization algorithm [111,127,128]. In some
378 cases, researchers can thus achieve state-of-the-art performance simply by investing large
379 computational budgets into tuning these types of factors for a specific test dataset. Consequently,
380 many of the currently reported DL benchmarks are built on top of massive computational budgets
381 and are often difficult to reproduce by other researchers without full access to the original code
382 and computing environments [110,111,126,129]. Recent empirical findings further suggest that
383 the comparisons performed on several of these benchmarks lack the statistical power required to
384 accurately determine the reported improvements in model performance [130], a problem similarly
385 evident in neuroimaging research [131].

386 In addition to these challenges for the reproducibility of benchmark model performances,
387 recent findings have also demonstrated that the resulting highly tuned models often lack basic
388 robustness towards slight distributional shifts [112,113,115-117,132] or corruptions [121,133] of
389 the data, while model performances can also vary widely across the different subpopulations of a
390 dataset (stratified, for example, by people’s age, race or gender; [134]) or be based in spurious
391 shortcuts that the models have learned from a training dataset but which do not generalize well to
392 other scenarios [52,118].

393 For these reasons, researchers have started advocating for more comprehensive and
394 standardized reporting of the training history of DL models [135], more extensive evaluation
395 procedures [112-115,136], as well as an increased scientific rigor in DL research [123]. In the
396 following, we briefly outline several recommendations resulting from this work, which aim to
397 improve the reproducibility and robustness of model performances (for a brief overview, see Box
398 4).

399 Most DL training pipelines are too complex to allow for a comprehensive evaluation of all
400 possible choices of hyper-parameters and other non-deterministic factors of the training. However,
401 evaluating only a specific instance of these choices does not give a reliable estimate of a model’s
402 expected performance in new data. Instead, recent empirical work suggests to randomize as many
403 of these choices as possible over multiple training runs, given the computational budget at hand
404 [136]. This allows to better account for the variance in model performance associated with these

405 choices and thus to obtain a more accurate estimate of the model's expected performance (see
406 [126,135,136]).

407 In addition, researchers have advocated for the use of multiple random splits of the data
408 into training, validation, and test datasets to evaluate model performances (e.g., with bootstrapping
409 or cross-validation; [109,136]). A single, predefined test dataset generally contains limited
410 information about the whole underlying data distribution and is thus also limited in its ability to
411 provide an accurate estimate of the model's expected performance in new data. Multiple random
412 splits, in contrast, better account for the variance in model performance associated with different
413 splits of the data, allowing to reduce the error in a model's expected performance.

414 Further, to ensure that the chosen combination of statistical comparison method and test
415 dataset size provides sufficient statistical power to accurately determine the studied difference in
416 model performance, researchers have recently suggested the use of simple simulation studies, by
417 first identifying and estimating the required quantities of the statistical testing procedure (e.g.,
418 McNemar's test for paired data requires the models' probabilities of making a correct prediction
419 as well as their agreement rate), and subsequently using these estimates to simulate model
420 comparisons at different dataset sizes [130]. In addition to ensuring that the chosen performance
421 evaluation procedure does not lack statistical power, recent work in neuroimaging also suggests to
422 control for multiple sequential model comparisons, as multiple sequential hypothesis tests (e.g.,
423 performance comparisons) on the same dataset can inflate false positive rates [137].

424 Next to choosing appropriate means of evaluating model performances in a given dataset,
425 it is essential to ensure that the resulting performances are robust towards real-world data (e.g.,
426 neuroimaging data from different individuals, tasks, and laboratories). Model performances can
427 falter, for example, when encountering slight distributional shifts or corruptions of the data, as
428 recently demonstrated by researchers who confronted benchmark DL models with datasets that
429 mimicked the original benchmarks but included new samples from the original data sources (thus
430 introducing distributional shifts; [79]) or by corrupting the inputs with simple noise [121,133]. To
431 strengthen robustness towards these types of scenarios, empirical work suggests the use of random
432 data augmentations during training, for example, by randomly flipping images from left-to-right
433 [138] or by randomly occluding [139] or mixing [140,141] inputs. It can also be beneficial to mix
434 different data augmentation strategies [142] or to automatically learn these strategies from the data
435 [143].

436 Similarly, DL model performances have been shown to often vary highly across the
437 different, often unrecognized, subpopulations of a dataset (a phenomenon known as “hidden
438 stratification”; [119,120]). For example, a DL model trained to distinguish benign and malignant
439 tumors from medical imaging data can perform well on average, while consistently misclassifying
440 an aggressive but rare form of cancer. To detect and measure these types of hidden stratification,
441 recent work suggests three approaches [119]: In schema completion, domain experts define and
442 provide a comprehensive set of subclasses for the test dataset (e.g., a more comprehensive labeling
443 of the cognitive states at different time points of the experiment), which can then be used to
444 evaluate the performance of models trained on the more coarsely-labeled training data. In error
445 auditing, domain experts retrospectively inspect instances of false model predictions to identify
446 possible hidden subpopulations (e.g., in combination with XAI techniques; see Box 1). In
447 automatic algorithmic approaches, dedicated algorithms independently search for hidden
448 subpopulations in the data and/or model predictions (e.g., by the use of clustering techniques).
449 Once hidden stratification is detected, modern DL techniques can be used to improve model
450 performances on subpopulations (e.g., [144]).

451 Lastly, it was demonstrated that DL models can be susceptible to learning spurious
452 shortcuts that allow them to perform well in a given training dataset but which do not generalize
453 well to other scenarios [52,118,122]. Researchers found, for example, that a pneumonia detection
454 model trained with medical imaging data can learn to perform well on average solely by learning
455 to identify hospital-specific artifacts in the medical images in addition to learning the hospitals’
456 pneumonia prevalence rates [145]. To identify these types of shortcuts, researchers recommend to
457 evaluate model performances on out-of-distribution data, for example, on data from different
458 sources (e.g., neuroimaging data from different laboratories and individuals), and to inspect
459 instances of the data whenever out-of-distribution error rates are high relative to in-distribution
460 errors (e.g., with visual inspection and/or the application of XAI techniques; see Box 1).

461
462 **Box 4. Recommendations to improve the reproducibility and robustness of DL modelling results in cognitive**
463 **decoding.**

464 The performances of DL models in benchmarks are often difficult to reproduce by other researchers or in new data, as
465 the convergence of DL models (and thereby their final performance) is strongly dependent on many non-deterministic
466 aspects of the training [110,111,135,136]. Further, the resulting highly tuned benchmark performances are often not
467 robust towards the diversity of real-world data [79,112-116]. Below, we provide a set of general recommendations to
468 improve the reproducibility and robustness of DL model performances in cognitive decoding analyses:

- 469 ◇ Use multiple training runs to estimate a model's expected performance, given the computational budget at hand
470 (for methodological suggestions on how to estimate a model's expected performance (or to perform model
471 comparisons) based on multiple training runs, see [126,135,136]).
- 472 ◇ Apply random augmentations to the data during training, such as random occlusions [139] and combinations
473 [140,141] of the inputs.
- 474 ◇ For each training run, randomize as many aspects of the training pipeline as possible (including random seeds,
475 random weight initializations, and random shufflings of the training data) and use a random split of the data into
476 training, validation, and test datasets (e.g., by the use of bootstrapping or cross-validation; [109,136]).
- 477 ◇ If model comparisons are performed, ensure that the chosen combination of statistical comparison procedure and
478 test dataset size has enough statistical power to accurately determine the studied differences in model performance
479 (e.g., by the use of simple simulation studies; see [130]).
- 480 ◇ Whenever possible, evaluate model performances on out-of-distribution data (e.g., by using neuroimaging data
481 from different laboratories and individuals) and test for hidden stratification [119,120] by the use of schema
482 completion, error auditing or automatic algorithmic approaches (for methodological details, see [119]).
- 483 ◇ Finally, publicly share any used data, analysis code, and computing environment (e.g., by the use of containerization
484 with Docker or Singularity) in a dedicated repository (e.g., Open Science Framework; [146]).

485

486 Concluding remarks

487 DL methods have experienced great success in research and industry and have had major
488 impacts on society [1]. This success has triggered interest in their application to the field of
489 cognitive decoding, where researchers aim to characterize the representations of different brain
490 regions by identifying the set of cognitive states that can be accurately decoded (or identified) from
491 the activity of these regions. DL methods hold a high promise to revolutionize cognitive decoding
492 analyses with their unmatched ability to learn versatile representations of complex data. Yet, fully

493 leveraging the potential of DL methods in cognitive decoding is currently hindered by three main
494 challenges, which result from a general lack of interpretability of DL methods as well as difficulties
495 in applying them to small datasets and in ensuring their reproducibility and robustness.

496 Here, we have provided a detailed discussion of these three challenges and proposed a set
497 of solutions that are informed by recent advances in functional neuroimaging and machine learning
498 research. In sum, we recommend that researchers utilize XAI techniques to identify the mapping
499 between cognitive states and brain activity that a DL model has learned (Box 1-2), improve the
500 performance of DL methods in conventional neuroimaging datasets by pre-training these models
501 on public neuroimaging data (Box 3), and follow a set of specific recommendations to improve
502 the reproducibility and robustness of DL model performances (Box 4). We hope that researchers
503 will take inspiration from our discussion and explore the many open research questions that remain
504 on the path to determining whether DL methods can live up to their promise for cognitive
505 decoding.

506 Acknowledgments

507 Armin W. Thomas is supported by Stanford Data Science through the Ram and Vijay
508 Shriram Data Science Fellowship. Russell A. Poldrack is supported by the National Science
509 Foundation under Grant No. OAC-1760950. Christopher Ré gratefully acknowledges the support
510 of NIH under No. U54EB020405 (Mobilize), NSF under Nos. CCF1763315 (Beyond Sparsity),
511 CCF1563078 (Volume to Velocity), and 1937301 (RTML); ONR under No. N000141712266
512 (Unifying Weak Supervision); the Moore Foundation, NXP, Xilinx, LETI-CEA, Intel, IBM,
513 Microsoft, NEC, Toshiba, TSMC, ARM, Hitachi, BASF, Accenture, Ericsson, Qualcomm, Analog
514 Devices, the Okawa Foundation, American Family Insurance, Google Cloud, Salesforce, Total,
515 the HAI-AWS Cloud Credits for Research program, Stanford Data Science, and members of the
516 Stanford DAWN project: Facebook, Google, and VMWare. The Mobilize Center is a Biomedical
517 Technology Resource Center, funded by the NIH National Institute of Biomedical Imaging and
518 Bioengineering through Grant P41EB027060. The U.S. Government is authorized to reproduce
519 and distribute reprints for Governmental purposes notwithstanding any copyright notation thereon.
520 Any opinions, findings, and conclusions or recommendations expressed in this material are those

521 of the authors and do not necessarily reflect the views, policies, or endorsements, either expressed
522 or implied, of NIH, ONR, or the U.S. Government.

523 References

- 524 [1] Goodfellow, I. et al. (2016). Deep learning. MIT press.
- 525 [2] Livezey, J. A. and Glaser, J. I. (2021). Deep learning approaches for neural decoding across
526 architectures and recording modalities. *Briefings in bioinformatics*, 22(2), 1577-1591. doi:
527 10.1093/bib/bbaa355.
- 528 [3] Norman, K. A. et al. (2006). Beyond mind-reading: multi-voxel pattern analysis of fMRI
529 data. *Trends in cognitive sciences*, 10(9), 424-430. doi: 10.1016/j.tics.2006.07.005.
- 530 [4] Poldrack, R. A et al. (2015). Long-term neural and physiological phenotyping of a single
531 human. *Nature communications*, 6(1), 1-15. doi: 10.1038/ncomms9885.
- 532 [5] Tavor, I., et al. (2016). Task-free MRI predicts individual differences in brain activity
533 during task performance. *Science*, 352(6282), 216-220. doi: 10.1126/science.aad8127.
- 534 [6] Cole, M. W. et al. (2014). Intrinsic and task-evoked network architectures of the human
535 brain. *Neuron*, 83(1), 238-251. doi: 10.1016/j.neuron.2014.05.014.
- 536 [7] Gunning, D. et al. (2019). XAI—Explainable artificial intelligence. *Science Robotics*,
537 4(37). doi: 10.1126/scirobotics.aay7120.
- 538 [8] Samek, W et al. (2021). Explaining deep neural networks and beyond: A review of methods
539 and applications. *Proceedings of the IEEE*, 109(3), 247-278. doi:
540 10.1109/JPROC.2021.3060483.
- 541 [9] Doshi-Velez, F. and Kim, B. (2017). Towards a rigorous science of interpretable machine
542 learning. arXiv preprint arXiv:1702.08608. Available: <http://arxiv.org/abs/1702.08608>
- 543 [10] Montavon, G. et al. (2018). Methods for interpreting and understanding deep neural
544 networks. *Digital Signal Processing*, 73, 1-15. doi: 10.1016/j.dsp.2017.10.011.
- 545 [11] Nguyen, A. et al. (2016). Synthesizing the preferred inputs for neurons in neural networks
546 via deep generator networks. *Advances In Neural Information Processing Systems*, 29,
547 3387-3395. Available: [http://papers.nips.cc/paper/6519-synthesizing-the-preferred-inputs-](http://papers.nips.cc/paper/6519-synthesizing-the-preferred-inputs-for-neurons-in-neural-networks-via-deep-generator-networks.pdf)
548 [for-neurons-in-neural-networks-via-deep-generator-networks.pdf](http://papers.nips.cc/paper/6519-synthesizing-the-preferred-inputs-for-neurons-in-neural-networks-via-deep-generator-networks.pdf)
- 549 [12] Simonyan, K. et al. (2013). Deep inside convolutional networks: Visualising image

- 550 classification models and saliency maps. arXiv preprint arXiv:1312.6034. Available:
551 <http://arxiv.org/abs/1312.6034>
- 552 [13] Bach, S. et al. (2015). On pixel-wise explanations for non-linear classifier decisions by
553 layer-wise relevance propagation. PloS one, 10(7), e0130140. doi:
554 10.1371/journal.pone.0130140.
- 555 [14] Smilkov, D. et al. (2017). Smoothgrad: removing noise by adding noise. arXiv preprint
556 arXiv:1706.03825. Available: <http://arxiv.org/abs/1706.03825>
- 557 [15] Sundararajan, M. et al. (2017). Axiomatic attribution for deep networks. In International
558 Conference on Machine Learning (ICML), 70, 3319-3328. PMLR. Available:
559 <http://proceedings.mlr.press/v70/sundararajan17a.html>
- 560 [16] Shrikumar, A. et al. (2017). Learning important features through propagating activation
561 differences. In International Conference on Machine Learning (ICML), 70, 3145-3153.
562 PMLR. Available: <http://proceedings.mlr.press/v70/shrikumar17a.html>
- 563 [17] Springenberg, J. T. et al. (2014). Striving for simplicity: The all convolutional net. arXiv
564 preprint arXiv:1412.6806. Available: <http://arxiv.org/abs/1412.6806>
- 565 [18] Selvaraju, R. R. et al. (2017). Grad-cam: Visual explanations from deep networks via
566 gradient-based localization. IEEE international conference on computer vision (ICCV),
567 618-626. Available:
568 [https://openaccess.thecvf.com/content_iccv_2017/html/Selvaraju_Grad-](https://openaccess.thecvf.com/content_iccv_2017/html/Selvaraju_Grad-CAM_Visual_Explanations_ICCV_2017_paper.html)
569 [CAM_Visual_Explanations_ICCV_2017_paper.html](https://openaccess.thecvf.com/content_iccv_2017/html/Selvaraju_Grad-CAM_Visual_Explanations_ICCV_2017_paper.html)
- 570 [19] Kindermans, P. J. et al. (2017). Learning how to explain neural networks: Patternnet and
571 patternattribution. arXiv preprint arXiv:1705.05598. Available:
572 <http://arxiv.org/abs/1705.05598>
- 573 [20] Fong, R. C. and Vedaldi, A. (2017). Interpretable explanations of black boxes by
574 meaningful perturbation. IEEE international conference on computer vision (ICCV), 3429-
575 3437. Available:
576 [https://openaccess.thecvf.com/content_iccv_2017/html/Fong_Interpretable_Explanations_o](https://openaccess.thecvf.com/content_iccv_2017/html/Fong_Interpretable_Explanations_of_ICCV_2017_paper.html)
577 [f_ICCV_2017_paper.html](https://openaccess.thecvf.com/content_iccv_2017/html/Fong_Interpretable_Explanations_of_ICCV_2017_paper.html)
- 578 [21] Montavon, G. et al. (2017). Explaining nonlinear classification decisions with deep taylor
579 decomposition. Pattern Recognition, 65, 211-222. doi: 10.1016/j.patcog.2016.11.008.
- 580 [22] Zurada, J. M. et al. (1994). Sensitivity analysis for minimization of input data dimension for

- 581 feedforward neural network. IEEE International Symposium on Circuits and Systems-
582 ISCAS'94, 6, 447-450 doi: 10.1109/ISCAS.1994.409622.
- 583 [23] Lundberg, S. M. and Lee, S. I. (2017). A unified approach to interpreting model
584 predictions. *Advances in Neural Information Processing Systems*, 30, 4768-4777.
585 Available:
586 [https://proceedings.neurips.cc/paper/2017/file/8a20a8621978632d76c43dfd28b67767-](https://proceedings.neurips.cc/paper/2017/file/8a20a8621978632d76c43dfd28b67767-Paper.pdf)
587 [Paper.pdf](https://proceedings.neurips.cc/paper/2017/file/8a20a8621978632d76c43dfd28b67767-Paper.pdf)
- 588 [24] Zeiler M.D. and Fergus R. (2014) Visualizing and Understanding Convolutional Networks.
589 In: Fleet D. et al. (eds) *Computer Vision – ECCV 2014*. ECCV 2014. Lecture Notes in
590 Computer Science, vol 8689. Springer, Cham. [https://doi.org/10.1007/978-3-319-10590-](https://doi.org/10.1007/978-3-319-10590-1_53)
591 [1_53](https://doi.org/10.1007/978-3-319-10590-1_53)
- 592 [25] Zintgraf, L. M. et al. (2017). Visualizing deep neural network decisions: Prediction
593 difference analysis. arXiv preprint arXiv:1702.04595. Available:
594 <http://arxiv.org/abs/1702.04595>
- 595 [26] Ribeiro, M. T. et al. (2016). "Why should i trust you?" Explaining the predictions of any
596 classifier. *ACM SIGKDD international conference on knowledge discovery and data*
597 *mining*, 1135-1144. doi: 10.1145/2939672.2939778.
- 598 [27] Luong, T. et al. (2015). Effective Approaches to Attention-based Neural Machine
599 Translation. *Conference on Empirical Methods in Natural Language Processing (EMNLP)*,
600 1412–1421. doi: 10.18653/v1/D15-1166.
- 601 [28] Xu, K. et al. (2015). Show, attend and tell: Neural image caption generation with visual
602 attention. *International conference on machine learning (ICML)*, 37, 2048-2057. PMLR.
603 Available: <http://proceedings.mlr.press/v37/xuc15.html>
- 604 [29] Vaswani, A. et al. (2017). Attention is all you need. *Advances In Neural Information*
605 *Processing Systems*, 30, 5998-6008. Available:
606 <https://papers.nips.cc/paper/2017/file/3f5ee243547dee91fbd053c1c4a845aa-Paper.pdf>
- 607 [30] Kim, B. et al. (2018). Interpretability beyond feature attribution: Quantitative testing with
608 concept activation vectors (tcav). *International conference on machine learning (ICML)*, 80,
609 2668-2677. PMLR. Available: <http://proceedings.mlr.press/v80/kim18d.html>
- 610 [31] Alvarez-Melis, D. and Jaakkola, T. S. (2018, December). Towards robust interpretability
611 with self-explaining neural networks. *Advances in Neural Information Processing Systems*,

- 612 31, 7786-7795. Available:
613 <https://proceedings.neurips.cc/paper/2018/file/3e9f0fc9b2f89e043bc6233994dfcf76->
614 [Paper.pdf](#)
- 615 [32] Dinsdale, N. K. et al. (2021). Learning patterns of the ageing brain in MRI using deep
616 convolutional networks. *Neuroimage*, 224, 117401. doi:
617 10.1016/j.neuroimage.2020.117401.
- 618 [33] Oh, K. et al. (2019). Classification and visualization of Alzheimer's disease using
619 volumetric convolutional neural network and transfer learning. *Scientific Reports*, 9(1), 1-
620 16. doi: 10.1038/s41598-019-54548-6.
- 621 [34] Thomas, A. W. et al. (2019). Analyzing neuroimaging data through recurrent deep learning
622 models. *Frontiers in neuroscience*, 13, 1321. doi: 10.3389/fnins.2019.01321.
- 623 [35] Kohoutová, L. et al. (2020). Toward a unified framework for interpreting machine-learning
624 models in neuroimaging. *Nature protocols*, 15(4), 1399-1435. doi: 10.1038/s41596-019-
625 0289-5.
- 626 [36] Zhang, Y. et al. (2021). Functional annotation of human cognitive states using deep graph
627 convolution. *NeuroImage*, 231, 117847. doi: 10.1016/j.neuroimage.2021.117847.
- 628 [37] Wang, X. et al. (2020). Decoding and mapping task states of the human brain via deep
629 learning. *Human brain mapping*, 41(6), 1505-1519. doi: <https://doi.org/10.1002/hbm.24891>.
- 630 [38] Hu, J. et al. (2021). Deep learning-based classification and voxel-based visualization of
631 frontotemporal dementia and Alzheimer's disease. *Frontiers in Neuroscience*, 14, 1468. doi:
632 10.3389/fnins.2020.626154.
- 633 [39] Nguyen, S. et al. (2020). Attend and Decode: 4D fMRI Task State Decoding Using
634 Attention Models. *Machine Learning for Health*, 136, 267-279. PMLR. Available:
635 <http://proceedings.mlr.press/v136/nguyen20a.html>
- 636 [40] Zhang, T. et al. (2020). Separated channel attention convolutional neural network (SC-
637 CNN-attention) to identify ADHD in multi-site rs-fMRI dataset. *Entropy*, 22(8), 893. doi:
638 10.3390/e22080893.
- 639 [41] Petersen, S. E. and Posner, M. I. (2012). The attention system of the human brain: 20 years
640 after. *Annual review of neuroscience*, 35, 73-89. doi: 10.1146/annurev-neuro-062111-
641 150525.
- 642 [42] Jain, S. and Wallace, B. C. (2019). Attention is not explanation. arXiv preprint

- 643 arXiv:1902.10186. Available: <http://arxiv.org/abs/1902.10186>
- 644 [43] Serrano, S. and Smith, N. A. (2019). Is Attention Interpretable?. Annual Meeting of the
645 Association for Computational Linguistics, 2931-2951. doi: 10.18653/v1/P19-1282.
- 646 [44] Samek, W. et al. (2016). Evaluating the visualization of what a deep neural network has
647 learned. IEEE transactions on neural networks and learning systems, 28(11), 2660-2673.
648 doi: 10.1109/TNNLS.2016.2599820.
- 649 [45] Kindermans, P. J. et al. (2019). The (un) reliability of saliency methods. Explainable AI:
650 Interpreting, Explaining and Visualizing Deep Learning, 267-280. Springer, Cham. doi:
651 10.1007/978-3-030-28954-6_14.
- 652 [46] Sun, J. et al. (2020). Understanding image captioning models beyond visualizing attention.
653 arXiv preprint arXiv:2001.01037. Available: <http://arxiv.org/abs/2001.01037>
- 654 [47] Adebayo, J. et al. (2018). Sanity Checks for Saliency Maps. Advances in Neural
655 Information Processing Systems, 31, 9505-9515. Available:
656 [https://proceedings.neurips.cc/paper/2018/file/294a8ed24b1ad22ec2e7efea049b8737-](https://proceedings.neurips.cc/paper/2018/file/294a8ed24b1ad22ec2e7efea049b8737-Paper.pdf)
657 [Paper.pdf](https://proceedings.neurips.cc/paper/2018/file/294a8ed24b1ad22ec2e7efea049b8737-Paper.pdf)
- 658 [48] Jacovi, A. and Goldberg, Y. (2020). Towards faithfully interpretable NLP systems: How
659 should we define and evaluate faithfulness?. arXiv preprint arXiv:2004.03685. Available:
660 <http://arxiv.org/abs/2004.03685>
- 661 [49] Kohlbrenner, M. et al. (2020). Towards best practice in explaining neural network decisions
662 with LRP. International Joint Conference on Neural Networks (IJCNN), 1-7. IEEE. doi:
663 10.1109/IJCNN48605.2020.9206975.
- 664 [50] Montavon G. et al. (2019) Layer-Wise Relevance Propagation: An Overview. Samek, W. et
665 al. (eds) Explainable AI: Interpreting, Explaining and Visualizing Deep Learning. Lecture
666 Notes in Computer Science, 11700. Springer, Cham. doi: 10.1007/978-3-030-28954-6_10
- 667 [51] Hanson, S. J. et al. (2004). Combinatorial codes in ventral temporal lobe for object
668 recognition: Haxby (2001) revisited: is there a “face” area?. Neuroimage, 23(1), 156-166.
669 doi: 10.1016/j.neuroimage.2004.05.020.
- 670 [52] Lapuschkin, S. et al. (2019). Unmasking Clever Hans predictors and assessing what
671 machines really learn. Nature communications, 10(1), 1-8. doi: 10.1038/s41467-019-08987-
672 4.
- 673 [53] Bassett, D. S. and Sporns, O. (2017). Network neuroscience. Nature neuroscience, 20(3),

- 674 353-364. doi: 10.1038/nm.4502.
- 675 [54] Alber, M. et al. (2019). iNNvestigate neural networks!. *J. Mach. Learn. Res.*, 20(93), 1-8.
- 676 [55] Kokhlikyan, N. et al. (2020). Captum: A unified and generic model interpretability library
677 for pytorch. arXiv preprint arXiv:2009.07896. Available: <http://arxiv.org/abs/2009.07896>
- 678 [56] Ancona, M. et al. (2018). Towards better understanding of gradient-based attribution
679 methods for Deep Neural Networks. *International Conference on Learning Representations*.
680 doi: 10.5167/uzh-168590.
- 681 [57] Sturmfels, P. et al. (2020). Visualizing the impact of feature attribution baselines. *Distill*,
682 5(1), e22. doi: 10.23915/distill.00022.
- 683 [58] Simonyan, K. and Zisserman, A. (2014). Very deep convolutional networks for large-scale
684 image recognition. arXiv preprint arXiv:1409.1556. Available:
685 <http://arxiv.org/abs/1409.1556>
- 686 [59] Devlin, J. et al. (2018). Bert: Pre-training of deep bidirectional transformers for language
687 understanding. arXiv preprint arXiv:1810.04805. Available:
688 <http://arxiv.org/abs/1810.04805>
- 689 [60] Zeng, W. et al. (2021). PanGu- α : Large-scale Autoregressive Pretrained Chinese
690 Language Models with Auto-parallel Computation. arXiv preprint arXiv:2104.12369.
691 Available: <http://arxiv.org/abs/2104.12369>
- 692 [61] Raffel, C. et al. (2020). Exploring the Limits of Transfer Learning with a Unified Text-to-
693 Text Transformer. *Journal of Machine Learning Research*, 21, 1-67.
- 694 [62] Brown, T. et al. (2020). Language Models are Few-Shot Learners. *Advances in Neural*
695 *Information Processing Systems*, 33, 1877-1901. Available:
696 <https://papers.nips.cc/paper/2020/file/1457c0d6bfc4967418bfb8ac142f64a-Paper.pdf>
- 697 [63] Allen-Zhu, Z. et al. (2019) A convergence theory for deep learning via over-
698 parameterization. *International Conference on Machine Learning (ICML)*, 97, 242-252.
699 PMLR. Available: <http://proceedings.mlr.press/v97/allen-zhu19a.html>
- 700 [64] Li, Y. and Liang, Y. (2018). Learning overparameterized neural networks via stochastic
701 gradient descent on structured data. *Advances in Neural Information Processing Systems*,
702 8168-8177.
703 [https://proceedings.neurips.cc/paper/2018/file/54fe976ba170c19ebae453679b362263-](https://proceedings.neurips.cc/paper/2018/file/54fe976ba170c19ebae453679b362263-Paper.pdf)
704 [Paper.pdf](https://proceedings.neurips.cc/paper/2018/file/54fe976ba170c19ebae453679b362263-Paper.pdf)

- 705 [65] Kolesnikov A. et al. (2020) Big Transfer (BiT): General Visual Representation Learning.
706 Vedaldi, A. et al. (eds) Computer Vision – ECCV 2020. ECCV 2020. Lecture Notes in
707 Computer Science, 12350. Springer, Cham. https://doi.org/10.1007/978-3-030-58558-7_29
- 708 [66] Chen, T. et al. (2020). Big Self-Supervised Models are Strong Semi-Supervised Learners.
709 Advances in Neural Information Processing Systems, 33, 22243-22255. Available:
710 [https://proceedings.neurips.cc/paper/2020/file/fcbc95ccdd551da181207c0c1400c655-](https://proceedings.neurips.cc/paper/2020/file/fcbc95ccdd551da181207c0c1400c655-Paper.pdf)
711 [Paper.pdf](https://proceedings.neurips.cc/paper/2020/file/fcbc95ccdd551da181207c0c1400c655-Paper.pdf)
- 712 [67] Sun, C. et al. (2017). Revisiting unreasonable effectiveness of data in deep learning era.
713 IEEE international conference on computer vision (ICCV), 843-852. doi:
714 10.1109/ICCV.2017.97.
- 715 [68] Krogh, A. and Hertz, J. A. (1992). A simple weight decay can improve generalization.
716 Advances In Neural Information Processing Systems, 950-957. Available:
717 <http://papers.nips.cc/paper/563-a-simple-weight-decay-can-improve-generalization.pdf>
- 718 [69] Pascanu, R. et al. (2013). On the difficulty of training recurrent neural networks.
719 International conference on machine learning (ICML), 28, 1310-1318. PMLR. Available:
720 <http://proceedings.mlr.press/v28/pascanu13.html>
- 721 [70] Srivastava, N. et al. (2014). Dropout: a simple way to prevent neural networks from
722 overfitting. The journal of machine learning research, 15(1), 1929-1958.
- 723 [71] Pan, S. J. and Yang, Q. (2009). A survey on transfer learning. IEEE Transactions on
724 knowledge and data engineering, 22(10), 1345-1359. doi: 10.1109/TKDE.2009.191.
- 725 [72] Deng, J. et al. (2009). ImageNet: A large-scale hierarchical image database. IEEE
726 Conference on Computer Vision and Pattern Recognition (CVPR), 248-255. IEEE. doi:
727 10.1109/CVPR.2009.5206848.
- 728 [73] Bowman, S. R. et al. (2015). A large annotated corpus for learning natural language
729 inference. Conference on Empirical Methods in Natural Language Processing (EMNLP),
730 632-642. doi: 10.18653/v1/D15-1075.
- 731 [74] Deepak, S. and Ameer, P. M. (2019). Brain tumor classification using deep CNN features
732 via transfer learning. Computers in biology and medicine, 111, 103345. doi:
733 10.1016/j.combiomed.2019.103345.
- 734 [75] Bengio, Y. et al. (2007). Greedy layer-wise training of deep networks. Advances in neural
735 information processing systems, 19, 153-160. Available:

- 736 <https://papers.nips.cc/paper/2006/file/5da713a690c067105aeb2fae32403405-Paper.pdf>
- 737 [76] Erhan, D. et al. (2010). Why does unsupervised pre-training help deep learning?.
- 738 International conference on artificial intelligence and statistics, 9, 201-208. Available:
- 739 <http://proceedings.mlr.press/v9/erhan10a.html>
- 740 [77] Yosinski, J. et al. (2014). How transferable are features in deep neural networks?. Advances
- 741 In Neural Information Processing Systems, 27, 3320-3328. Available:
- 742 <http://papers.nips.cc/paper/5347-how-transferable-are-features-in-deep-neural-networks.pdf>
- 743 [78] Kornblith, S. et al. (2019). Do better imagenet models transfer better?. IEEE/CVF
- 744 Conference on Computer Vision and Pattern Recognition, 2661-2671. doi:
- 745 10.1109/CVPR.2019.00277.
- 746 [79] Recht, B. et al. (2019). Do imagenet classifiers generalize to imagenet?. International
- 747 Conference on Machine Learning (ICML), 97, 5389-5400. PMLR. Available:
- 748 <http://proceedings.mlr.press/v97/recht19a.html>
- 749 [80] He, K. et al. (2019). Rethinking imagenet pre-training. IEEE/CVF International Conference
- 750 on Computer Vision (ICCV), 4918-4927. doi: 10.1109/ICCV.2019.00502.
- 751 [81] Horien, C. et al. (2021). A hitchhiker's guide to working with large, open-source
- 752 neuroimaging datasets. Nature human behaviour, 5(2), 185-193. doi: 10.1038/s41562-020-
- 753 01005-4.
- 754 [82] Gorgolewski, K. J. et al. (2016). The brain imaging data structure, a format for organizing
- 755 and describing outputs of neuroimaging experiments. Scientific data, 3(1), 1-9. doi:
- 756 10.1038/sdata.2016.44.
- 757 [83] Markiewicz, C. J. et al. (2021). OpenNeuro: An open resource for sharing of neuroimaging
- 758 data. *bioRxiv*. doi: 10.1101/2021.06.28.450168.
- 759 [84] Esteban, O. et al. (2019). fMRIPrep: a robust preprocessing pipeline for functional MRI.
- 760 Nature methods, 16(1), 111-116. doi: 10.1038/s41592-018-0235-4.
- 761 [85] Mahmood, U. et al. (2019). Transfer learning of fMRI dynamics. arXiv preprint
- 762 arXiv:1911.06813. Available: <http://arxiv.org/abs/1911.06813>
- 763 [86] Koyamada, S. et al. (2015). Deep learning of fMRI big data: a novel approach to subject-
- 764 transfer decoding. arXiv preprint arXiv:1502.00093. Available:
- 765 <http://arxiv.org/abs/1502.00093>
- 766 [87] Zheng, W. L. et al. (2016). Personalizing EEG-based affective models with transfer

- 767 learning. International joint conference on artificial intelligence, 2732-2738.
- 768 [88] Thomas A.W. et al. (2019) Deep Transfer Learning for Whole-Brain fMRI Analyses.
769 Zhou L. et al. (eds) OR 2.0 Context-Aware Operating Theaters and Machine Learning in
770 Clinical Neuroimaging. OR 2.0 2019, MLCN 2019. Lecture Notes in Computer Science,
771 vol 11796. Springer, Cham. https://doi.org/10.1007/978-3-030-32695-1_7
- 772 [89] Zhang, H. et al. (2018). Transfer learning on fMRI datasets. International Conference on
773 Artificial Intelligence and Statistics, 84, 595-603. PMLR. Available:
774 <http://proceedings.mlr.press/v84/zhang18b.html>
- 775 [90] Yousefnezhad, M. et al. (2020). Shared Space Transfer Learning for analyzing multi-site
776 fMRI data. Advances in Neural Information Processing Systems, 33, 15990-16000.
777 [https://proceedings.neurips.cc/paper/2020/file/b837305e43f7e535a1506fc263eee3ed-](https://proceedings.neurips.cc/paper/2020/file/b837305e43f7e535a1506fc263eee3ed-Paper.pdf)
778 [Paper.pdf](https://proceedings.neurips.cc/paper/2020/file/b837305e43f7e535a1506fc263eee3ed-Paper.pdf)
- 779 [91] Mensch, A. et al. (2021). Extracting representations of cognition across neuroimaging
780 studies improves brain decoding. PLoS computational biology, 17(5), e1008795. doi:
781 10.1371/journal.pcbi.1008795.
- 782 [92] Zhou S. et al. (2019) Improving Whole-Brain Neural Decoding of fMRI with Domain
783 Adaptation. Suk, H. I. et al. (eds) Machine Learning in Medical Imaging. MLMI 2019.
784 Lecture Notes in Computer Science, vol 11861. Springer, Cham.
785 https://doi.org/10.1007/978-3-030-32692-0_31
- 786 [93] Turner, J. A. and Laird, A. R. (2012). The cognitive paradigm ontology: design and
787 application. Neuroinformatics, 10(1), 57-66. doi: 10.1007/s12021-011-9126-x.
- 788 [94] Poldrack, R. A. et al. (2011). The cognitive atlas: toward a knowledge foundation for
789 cognitive neuroscience. Frontiers in neuroinformatics, 5, 17. doi:
790 10.3389/fninf.2011.00017.
- 791 [95] Daneman, M. and Carpenter, P. A. (1980). Individual differences in working memory and
792 reading. Journal of verbal learning and verbal behavior, 19(4), 450-466. doi:
793 10.1016/S0022-5371(80)90312-6.
- 794 [96] Wechsler, D. (2008). Wechsler Adult Intelligence Scale--Fourth Edition. doi:
795 10.1037/t15169-000.
- 796 [97] Zhou, Z. H. (2018). A brief introduction to weakly supervised learning. National science
797 review, 5(1), 44-53. doi: 10.1093/nsr/nwx106.

- 798 [98] Ratner, A. J. et al. (2016). Data programming: Creating large training sets, quickly.
799 Advances In Neural Information Processing Systems, 29, 3567-3575. Available:
800 [https://proceedings.neurips.cc/paper/2016/file/6709e8d64a5f47269ed5cea9f625f7ab-](https://proceedings.neurips.cc/paper/2016/file/6709e8d64a5f47269ed5cea9f625f7ab-Paper.pdf)
801 [Paper.pdf](https://proceedings.neurips.cc/paper/2016/file/6709e8d64a5f47269ed5cea9f625f7ab-Paper.pdf)
- 802 [99] Ratner, A. et al. (2017). Snorkel: Rapid training data creation with weak supervision.
803 VLDB Endowment. International Conference on Very Large Data Bases, 11(3), 269. NIH
804 Public Access. doi: 10.14778/3157794.3157797.
- 805 [100] Dunnmon, J. A. et al. (2020). Cross-modal data programming enables rapid medical
806 machine learning. Patterns, 1(2), 100019. doi: 10.1016/j.patter.2020.100019.
- 807 [101] Bengio, Y. et al. (2013). Representation learning: A review and new perspectives. IEEE
808 transactions on pattern analysis and machine intelligence, 35(8), 1798-1828. doi:
809 10.1109/TPAMI.2013.50.
- 810 [102] Barlow, H. B. (1989). Unsupervised learning. Neural computation, 1(3), 295-311. doi:
811 10.1162/neco.1989.1.3.295.
- 812 [103] Liu, X. et al. (2021). Self-supervised learning: Generative or contrastive. IEEE
813 Transactions on Knowledge and Data Engineering. doi: 10.1109/TKDE.2021.3090866.
- 814 [104] Chen, T. et al. (2020). A simple framework for contrastive learning of visual
815 representations. International conference on machine learning (ICML), 119,1597-1607.
816 PMLR. Available: <http://proceedings.mlr.press/v119/chen20j.html>
- 817 [105] Hinton, G. E. et al. (2006). A fast learning algorithm for deep belief nets. Neural
818 computation, 18(7), 1527-1554. doi: 10.1162/neco.2006.18.7.1527.
- 819 [106] Kotsiantis, S. B. et al. (2007). Supervised machine learning: A review of classification
820 techniques. Emerging artificial intelligence applications in computer engineering, 160(1), 3-
821 24.
- 822 [107] Botvinik-Nezer, R. et al. (2020). Variability in the analysis of a single neuroimaging
823 dataset by many teams. Nature, 582(7810), 84-88. doi: 10.1038/s41586-020-2314-9.
- 824 [108] Bouthillier, X., et al. (2019). Unreproducible research is reproducible. International
825 Conference on Machine Learning (ICML), 97, 725-734. PMLR. Available:
826 <http://proceedings.mlr.press/v97/bouthillier19a.html>
- 827 [109] Gorman, K. and Bedrick, S. (2019). We need to talk about standard splits. Association for
828 computational linguistics, 2786-2791. doi: 10.18653/v1/P19-1267.

- 829 [110] Henderson, P. et al. (2018). Deep reinforcement learning that matters. AAAI conference
830 on artificial intelligence, 32(1). Available:
831 <https://ojs.aaai.org/index.php/AAAI/article/view/11694>
- 832 [111] Lucic, M. et al. (2018). Are GANs Created Equal? A Large-Scale Study. Advances In
833 Neural Information Processing Systems, 31. Available:
834 <https://papers.nips.cc/paper/2018/file/e46de7e1bcaaced9a54f1e9d0d2f800d-Paper.pdf>
- 835 [112] Koh, P. W. et al. (2021). Wilds: A benchmark of in-the-wild distribution shifts.
836 International Conference on Machine Learning (ICML), 139, 5637-5664. PMLR.
837 Available: <http://proceedings.mlr.press/v139/koh21a.html>
- 838 [113] Hendrycks, D. et al. (2020). The many faces of robustness: A critical analysis of out-of-
839 distribution generalization. arXiv preprint arXiv:2006.16241. Available:
840 <http://arxiv.org/abs/2006.16241>
- 841 [114] Kiela, D. et al. (2021). Dynabench: Rethinking Benchmarking in NLP. Conference of the
842 North American Chapter of the Association for Computational Linguistics: Human
843 Language Technologies, 4110-4124. doi: 10.18653/v1/2021.naacl-main.324.
- 844 [115] Goel, K. et al. (2021). Robustness Gym: Unifying the NLP Evaluation Landscape.
845 Conference of the North American Chapter of the Association for Computational
846 Linguistics: Human Language Technologies: Demonstrations, 42-55. doi:
847 10.18653/v1/2021.naacl-demos.6.
- 848 [116] Hendrycks, D. and Dietterich, T. (2019). Benchmarking neural network robustness to
849 common corruptions and perturbations. arXiv preprint arXiv:1903.12261. Available:
850 <http://arxiv.org/abs/1903.12261>
- 851 [117] Miller, J. et al. (2020). The effect of natural distribution shift on question answering
852 models. International Conference on Machine Learning (ICML), 119, 6905-6916. PMLR.
853 Available: <http://proceedings.mlr.press/v119/miller20a.html>
- 854 [118] Geirhos, R. et al. (2020). Shortcut learning in deep neural networks. Nature Machine
855 Intelligence, 2(11), 665-673. doi: 10.1038/s42256-020-00257-z.
- 856 [119] Oakden-Rayner, L. et al. (2020). Hidden stratification causes clinically meaningful
857 failures in machine learning for medical imaging. ACM conference on health, inference,
858 and learning, 151-159. doi: 10.1145/3368555.3384468.
- 859 [120] Sohoni, N. et al. (2020). No Subclass Left Behind: Fine-Grained Robustness in Coarse-

- 860 Grained Classification Problems. *Advances in Neural Information Processing Systems*, 33,
861 19339-19352. Available:
862 <https://papers.nips.cc/paper/2020/file/e0688d13958a19e087e123148555e4b4-Paper.pdf>
- 863 [121] Belinkov, Y. and Bisk, Y. (2017). Synthetic and natural noise both break neural machine
864 translation. *arXiv preprint arXiv:1711.02173*. Available: <http://arxiv.org/abs/1711.02173>
- 865 [122] McCoy, T. et al. (2019). Right for the Wrong Reasons: Diagnosing Syntactic Heuristics
866 in Natural Language Inference. *Annual Meeting of the Association for Computational*
867 *Linguistics*, 3428-3448. doi: 10.18653/v1/P19-1334.
- 868 [123] Lipton, Z. C. and Steinhardt, J. (2018). Troubling trends in machine learning scholarship.
869 *arXiv preprint arXiv:1807.03341*. Available: <http://arxiv.org/abs/1807.03341>
- 870 [124] Ethayarajh, K. and Jurafsky, D. (2020). Utility is in the Eye of the User: A Critique of
871 NLP Leaderboards. *Conference on Empirical Methods in Natural Language Processing*
872 (EMNLP), 4846–4853. doi: 10.18653/v1/2020.emnlp-main.393.
- 873 [125] Simmons, J. P. et al. (2011). False-positive psychology: Undisclosed flexibility in data
874 collection and analysis allows presenting anything as significant. *Psychological science*,
875 22(11), 1359-1366. doi: 10.1177/0956797611417632.
- 876 [126] Reimers, N. and Gurevych, I. (2017). Reporting Score Distributions Makes a Difference:
877 Performance Study of LSTM-networks for Sequence Tagging. *Conference on Empirical*
878 *Methods in Natural Language Processing (EMNLP)*, 338–348. doi: 10.18653/v1/D17-1035.
- 879 [127] Melis, G. et al. (2017). On the state of the art of evaluation in neural language models.
880 *arXiv preprint arXiv:1707.05589*. Available: <http://arxiv.org/abs/1707.05589>
- 881 [128] Zoph, B. and Le, Q. V. (2016). Neural architecture search with reinforcement learning.
882 *arXiv preprint arXiv:1611.01578*. Available: <http://arxiv.org/abs/1611.01578>
- 883 [129] Raff, E. (2019). A step toward quantifying independently reproducible machine learning
884 research. *Advances in Neural Information Processing Systems*, 32, 5485-5495. Available:
885 [https://proceedings.neurips.cc/paper/2019/file/c429429b1f2af051f2021dc92a8ebeat-](https://proceedings.neurips.cc/paper/2019/file/c429429b1f2af051f2021dc92a8ebeat-Paper.pdf)
886 [Paper.pdf](https://proceedings.neurips.cc/paper/2019/file/c429429b1f2af051f2021dc92a8ebeat-Paper.pdf)
- 887 [130] Card, D. et al. (2020). With Little Power Comes Great Responsibility. *Conference on*
888 *Empirical Methods in Natural Language Processing (EMNLP)*, 9263–9274. doi:
889 10.18653/v1/2020.emnlp-main.745.
- 890 [131] Button, K. S. et al. (2013). Power failure: why small sample size undermines the

- 891 reliability of neuroscience. *Nature reviews neuroscience*, 14(5), 365-376. doi:
892 10.1038/nrn3475.
- 893 [132] Zheng, S. et al. (2016). Improving the robustness of deep neural networks via stability
894 training. *IEEE conference on computer vision and pattern recognition (CVPR)*, 4480-4488.
895 doi: 10.1109/CVPR.2016.485.
- 896 [133] Dodge, S. and Karam, L. (2017). A study and comparison of human and deep learning
897 recognition performance under visual distortions. *International conference on computer
898 communication and networks (ICCCN)*, 1-7. IEEE. doi: 10.1109/ICCCN.2017.8038465
- 899 [134] Buolamwini, J. and Gebru, T. (2018). Gender shades: Intersectional accuracy disparities
900 in commercial gender classification. *Conference on fairness, accountability and
901 transparency*, 81, 77-91. PMLR. Available:
902 <http://proceedings.mlr.press/v81/buolamwini18a.html>
- 903 [135] Dodge, J. et al. (2019). Show Your Work: Improved Reporting of Experimental Results.
904 2019 Conference on Empirical Methods in Natural Language Processing and the 9th
905 International Joint Conference on Natural Language Processing (EMNLP-IJCNLP), 2185-
906 2194. doi: 10.18653/v1/D19-1224.
- 907 [136] Bouthillier, X. et al. (2021). Accounting for variance in machine learning benchmarks.
908 *Machine Learning and Systems*, 3, 747-769. Available:
909 [https://proceedings.mlsys.org/paper/2021/file/cfecdb276f634854f3ef915e2e980c31-](https://proceedings.mlsys.org/paper/2021/file/cfecdb276f634854f3ef915e2e980c31-Paper.pdf)
910 [Paper.pdf](https://proceedings.mlsys.org/paper/2021/file/cfecdb276f634854f3ef915e2e980c31-Paper.pdf)
- 911 [137] Thompson, W. H. et al. (2020). Meta-research: Dataset decay and the problem of
912 sequential analyses on open datasets. *Elife*, 9, e53498. doi: 10.7554/eLife.53498.
- 913 [138] He, K. et al. (2016). Deep residual learning for image recognition. *IEEE conference on
914 computer vision and pattern recognition (CVPR)*, 770-778. doi: 10.1109/CVPR.2016.90.
- 915 [139] DeVries, T. and Taylor, G. W. (2017). Improved regularization of convolutional neural
916 networks with cutout. *arXiv preprint arXiv:1708.04552*. Available:
917 <http://arxiv.org/abs/1708.04552>
- 918 [140] Yun, S. et al. (2019). Cutmix: Regularization strategy to train strong classifiers with
919 localizable features. *IEEE/CVF International Conference on Computer Vision (ICCV)*,
920 6023-6032. doi: 10.1109/ICCV.2019.00612.
- 921 [141] Zhang, H. et al. (2017). Mixup: Beyond empirical risk minimization. *arXiv preprint*

- 922 arXiv:1710.09412. Available: <http://arxiv.org/abs/1710.09412>
- 923 [142] Hendrycks, D. et al. (2019). Augmix: A simple data processing method to improve
924 robustness and uncertainty. arXiv preprint arXiv:1912.02781. Available:
925 <http://arxiv.org/abs/1912.02781>
- 926 [143] Cubuk, E. D. et al. (2019). Autoaugment: Learning augmentation strategies from data.
927 IEEE/CVF Conference on Computer Vision and Pattern Recognition (CVPR), 113-123.
928 doi: 10.1109/CVPR.2019.00020.
- 929 [144] Sagawa, S. et al. (2019). Distributionally robust neural networks for group shifts: On the
930 importance of regularization for worst-case generalization. arXiv preprint
931 arXiv:1911.08731. Available: <http://arxiv.org/abs/1911.08731>
- 932 [145] Zech, J. R. et al. (2018). Variable generalization performance of a deep learning model to
933 detect pneumonia in chest radiographs: a cross-sectional study. PLoS medicine, 15(11),
934 e1002683. doi: 10.1371/journal.pmed.1002683.
- 935 [146] Foster, E. D. and Deardorff, A. (2017). Open science framework (OSF). Journal of the
936 Medical Library Association: JMLA, 105(2), 203. doi: 10.5195/jmla.2017.88.